

Nickel Nanoparticles to Enhance Heavy Crude Oil Recovery in Sudan Oil Plant

M. S. Suliman¹  , Sahl Yasin*²  , Basant Lal³  

¹ Lab analyst assistant, Petroenergy E&P Co., Ltd. Khartoum, Sudan.

² Sudanese chemical society Khartoum, Khartoum, Sudan

³ Department of Chemistry, Institute of Applied Science and Humanities, GLA University, Mathura-281406, India.

*Corresponding Author.

Received 06/06/2023, Revised 31/05/2024, Accepted 02/06/2024, Published Online First 20/09/2024



© 2022 The Author(s). Published by College of Science for Women, University of Baghdad.

This is an open access article distributed under the terms of the [Creative Commons Attribution 4.0 International License](https://creativecommons.org/licenses/by/4.0/), which permits unrestricted use, distribution, and reproduction in any medium, provided the original work is properly cited.

Abstract

This study focuses on the fabrication of nickel nanoparticles (Ni NPs) using a chemical reduction method with hydrazine monohydrate as the reducing agent. The Ni NPs were characterized using transmission electron microscopy (TEM) and X-ray diffraction spectrometry (XRD). The characterization results confirmed the production of pure Ni NPs with an average particle size ranging from 50 to 90 nm and various shapes depending on the hydrazine ratio. The synthesized Ni NPs were then utilized to enhance the viscosity reduction of heavy oil. Significant viscosity reduction of 51%, from 7128 mPa.s to 3495 mPa.s, was achieved at a temperature of 80 °C. Additionally, a slight decrease in density from 0.9514 g/cm³ to 0.9416 g/cm³ and a slight increase in the (American petroleum institute) API number from 17.04 to 18.59 (9.0%) were observed

Keywords: Morphology, Nickel nanoparticles, Oil viscosity, Sudan oil plant, XRD analysis.

Introduction

Frequently, global energy requirements describe our displays into the making and regulation of heavy crude oil (HCO), confirming the necessity for efficient HCO spill preparation and replies ¹. Unsimilar to common fuels, HCO controls a large viscosity, and density, includes high contents of resistant asphaltenes and pitches and can create catastrophic problems when dropped into the environment ². Biodegradation is an effective and environmentally eco-friendly choice for lost oil reduction ^{3,4, 5}. Investigations on the viscosity reduction of HCO are insufficient. The extremely viscous and dense HCO could fasten to the neighboring environments, such as plugging the pipelines and rock holes and precipitating and connecting to the trash ⁶. The idea and the concept behind nanotechnology started after Richard Feynman famous lecture at the American Physical Society meeting in 1959 ⁷. The preparation of nanomaterials from metals such as gold, silver, iron,

zinc, and copper started early and continues to the present ⁸. Nickel has two manifestations of nanoparticles: nickel metal (Ni) and nickel oxide (NiO). Both of these categories of nanoparticles have magnetic properties, antimicrobial activity, catalytic activity, and sorption nature and are biocompatible. Above all usage, NiO-NPs have exploited a semiconductor with high chemical stability and electron transferability and a band gap between 3.6 and 4.9 eV ⁹.

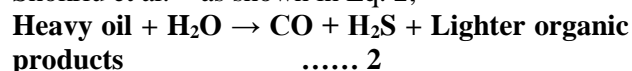
The general method to obtain pure nickel nanoparticles by a chemical mean and adopted by hydrazine as a reduced agent is described in Eq. 1.

Nickel salt + Solvent + reducing agent → Nickel nanoparticles..... 1

The reaction takes place under stirrer and reflux for two hours and temperature between 40-60 °C. Among all solvents, acetonitrile, ethanol, methanol, water dimethylsulphoxide, ethylene glycol, and cyclohexane are suitable for preparing nickel

nanoparticles. In such a way, Shokrdu et al. synthesized nickel nanoparticles and benzil diethylenetriamine and hydrazine were added as reducing agents at room temperature^{10,11, 12}. Nowadays, metal nanoparticles are employed in the oil industry, which is confirmed to be a great agent for recovering heavy oil. Heavy oil comprises substantial amounts of asphaltene and resin as major components with a high average molecular weight. Various nanoparticles have demonstrated their efficacy in enhancing oil recovery, and among them are commonly found in aluminum, zinc, magnesium, iron, zirconium, nickel, tin, and silicon oxides. These nanoparticle types have shown the potential to improve the efficiency of oil recovery processes. Therefore, the viscosity and density of the oil will shift to a high rate, have a very poor flow rate, and hence be very difficult to transport. The oil recovery technique stands on three basic processes: (i) primary process (using geological resident), (ii) secondary process (water flooding), and (iii) tertiary processes (enhanced oil recovery). The experiment of Shokrlu and his co-workers showed that the tertiary process is implemented and widely used when the water-to-oil ratio decreases. Hot water steam injection can lower oil viscosity and increase its mobility. Therefore, the aqua thermolysis reaction mechanism describes the transformation of heavy oil to light products at high temperatures. During this process, some of the sulfur/carbon bonds of organosulfur

broken, as described by the equation proposed by Shokrlu et al.¹² as shown in Eq. 2;



The carbon monoxide produced in the above reaction interacts with water molecules and fabricates carbon dioxide and hydrogen, while the dissociation of carbon dioxide can further reduce heavy oil viscosity¹³⁻¹⁵

Many studies were carried out to describe the role of trace metal nanoparticles as a catalyst for recovering heavy oil. Shakir and his co-author conducted a study using Nanosilica (NS) to upgrade Iraqi heavy crude oil and enhance solvent deasphalting. The results demonstrated a significant reduction in asphaltene quantities by 87.22%, increasing API to 35.9. Moreover, the process led to the completely removal of sulfur, vanadium, and nickel from the heavy oil.¹⁶

In this way, a chemical reduction procedure was exploited to obtain pure nickel nanoparticles from in ethanolic NiCl₂ solution, while hydrazine with different ratios was used as a reducing agent. The main aim of this study is to synthesize nickel nanoparticles by using hydrazine as a reducing agent and sodium hydroxide as solvent at 60 °C without using inert gas and adding surfactant agents. The obtained nanoparticles were characterized. Then, a comprehensive study was carried out on applying the synthesized nanoparticles to produce lighter crude oil with high quality from heavy crude oil.

Materials and Methods

Sampling

Crude oil samples were collected in triplicate from Unity, representing three wells from Al-Fulla region approximately (800 km from Khartoum), Western Sudan (west Kurdufan state). Fig. 1 showed samples

location. Ten samples were taken from different head tubing of wells. The samples were placed in vessels with screw caps. After that, the samples were transported to the lab.

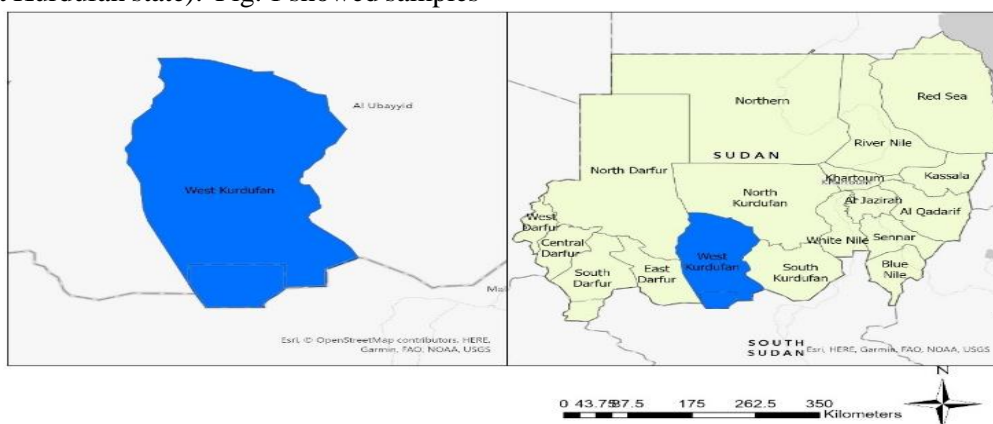


Figure 1. Samples location

Synthesis of Nickel nanoparticles (Ni NPs)

Nickel chloride hexahydrate ($\text{NiCl}_2 \cdot 6\text{H}_2\text{O}$), sodium hydroxide (NaOH), ethanol, and 80 wt.% hydrazine monohydrate ($\text{N}_2\text{H}_4 \cdot \text{H}_2\text{O}$), which were obtained from Sigma-Aldrich, were used to prepare nickel nanoparticles Ni NPs as described elsewhere by Ammare et al.¹⁰ In two separate beakers, an equal amount of nickel chloride hexahydrate (3 g) was dissolved in 25 ml of ethanol and added to two different amounts of hydrazine monohydrate $\text{N}_2\text{H}_4 \cdot \text{H}_2\text{O}$ (5.4 g and 8.2 g). Additionally, 4.38 g of sodium hydroxide was dissolved in 25 ml of ethanol and added to the same two beakers. The ratios between nickel and hydrazine were determined to be 1:10 and 1:15, respectively, and these mixtures were labeled as NPs-1 and NPs-2. The temperature was

maintained at 60 °C with continuous stirring to produce nickel nanoparticles, and the reaction was represented by eq 3. The formation of nanoparticles began early in the process. As illustrated in Fig. 2, the mixture initially changed to turquoise Fig. 2a, then after 2 minutes, it transitioned to grey Fig. 2B, and finally turned black Fig. 2C. After one hour, the resulting precipitate was collected using a 0.45 μm filter and subsequently washed with absolute ethanol, doubly-distilled water, and acetone. The black precipitate was dried at room temperature and stored in a sealed container for further analysis. The reaction can be expressed as shown in Eq. 3⁷.

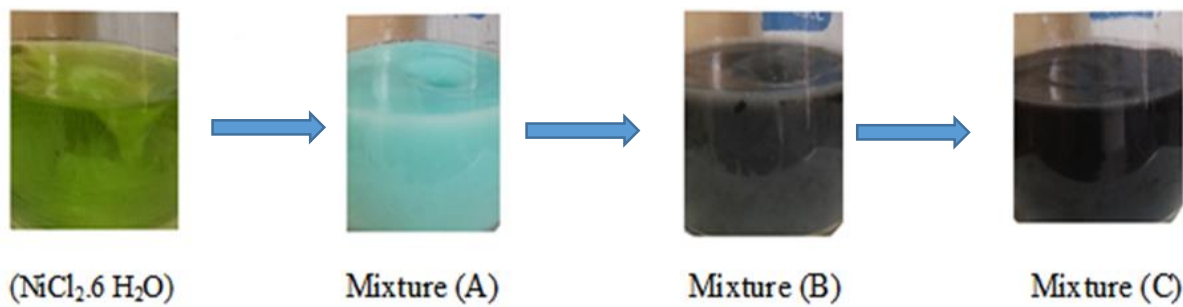
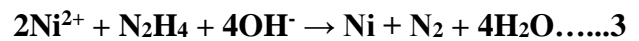


Figure 2. Preparation of nickel nanoparticles. Mixture 2A after 2 minutes 2B, mixture after half hour 2C

Characterization

The prepared Ni NPs samples were characterized by X-ray diffraction (XRD) exploiting PANalytical 3 kW X'pert Multifunctional diffractometer with $\text{Cu K}\alpha$ radiation source ($\lambda=0.1594$ nm). A step size of 0.0262° was used and patterns were recorded for 2θ values in the $20\text{-}120^\circ$ span. However, the average crystal sizes of the fabricated nanoparticles were computed from the full width at half maximum of the most intense reflection of metallic nickel, employing the Scherrer relation. For the (1 1 1), (2 0 0), (2 2 0) diffraction peak, based on the Scherrer relation, can be presented as Eq. 4;

$$d = \frac{K\lambda}{\beta} \cos \theta \quad \dots 4$$

where K is the Scherrer constant (0.89) related to the shape and index (h, k, l) of the crystal, d is the grain size, β is the corrected full width at half maximum (in radians), λ is the wavelength of the X-rays, and θ is the diffraction angle.

A transmission electron microscope (TEM) was utilized to determine the particle-size of the nanoparticles. The image was measured by H700H type transmission electron microscope Thermo Fisher Scientific at 80 kV with a resolution of 0.1 nm.

Effect of Ni NPs on Crude Oil Rheology

Nickel nanoparticles Ni NPs were applied to enhance heavy crude oil. The experiments were carried out by adding 0.05 g (0.5 %) of Ni NPs to 100 mL of crude oil at 80°C for 24 hours with continuous stirring. The percentage of the reduction of the oil viscosity samples ($\Delta\eta\%$) was calculated as shown in Eq. 5;

$$\Delta\eta = \left[\left(\frac{\eta_0 - \eta}{\eta_0} \right) \times 100 \right] \dots 5$$

where η_0 is the viscosity of the oil before the reaction (mPa.s), η is the viscosity of the oil after the reaction (mPa.s), and $\Delta\eta$ is the rate of viscosity reduction¹⁷.

Results and discussion

The Effects of Reducing Agent (N_2H_4) on Ni NPs Formation

The impact of reducing agent concentration on the synthesis of nickel nanoparticles was evaluated in this study. Ethanol was utilized as the solvent without the presence of a capping agent. The molar ratios of N_2H_4 to Ni^{2+} were 10:1 and 15:1, respectively, while the molar ratio of NaOH to Ni^{2+} was 10:1. The reaction temperature was elevated to 60 °C, leading to the rapid formation of black precipitates. The reaction was completed in less than 5 minutes, demonstrating its efficiency. These findings align with previous studies that have reported similar results^{18, 19}. Wu et al⁴. results displayed that, with increasing ratio of N_2H_4 -OH/ $NiCl_2$ diameter between atom amendments. When the percentage became bigger than 12 it became stable. The ratio of $N_2H_4:Ni^{2+}$ effect directly on the morphology of Nickel nanoparticles. Low hydrazine concentrations obtained large particles due to the slow creation of nuclei and seeds that colluded with nickel ions⁴. The formation of a stable nucleus requires the minimum number of atoms to form a proper collision.

X-ray Diffraction XRD

XRD results illustrate the patterns of nickel nanoparticles Ni NPs synthesized using varying molar ratios of $N_2H_4:Ni^{2+}$. In the case of the molar

ratio NPs-1 10:1 shown in Fig. 3, three distinct diffraction peaks were observed at 44.46°, 51.9°, and 76.4°. Among these, the peak with the highest intensity occurred at $2\theta = 44.57^\circ$. The corresponding Miller indices (111) and (200) confirmed that the resulting powders exhibited a face-centered cubic (FCC) crystal structure characteristic of nickel. For the molar ratio of NP-2 15:1 Fig. 3, three distinct diffraction peaks at 44.58°, 51.70°, and 76.39° were also observed. The highest intensity at 2θ was 44.52°. Their corresponding miller indices (111) and (200) confirm that the resulting powders were face-centered cubic (FCC) nickel. No other species were observed in the XRD pattern, indicating that pure nickel powders were in these experiments. The XRD pattern matches with the Joint Committee on Powder Diffraction Standards database (JCPDS PDF No.:04-0850), confirming the random powdered nickel arrangement. The finding of this technique is agreed with other literature; Goswami et al²⁰. synthesized nickel nanoparticles by adopting platinum chloride as the reducing agent and sodium hydroxide as the main solvent. They applied their technique for Oxygen Reduction and Formic Acid Oxidation Reactions. The XRD results showed that the main peaks observed at 44.4° correspond to the (111) crystalline plane of FCC lattice of cubic Ni NPs.²⁰.

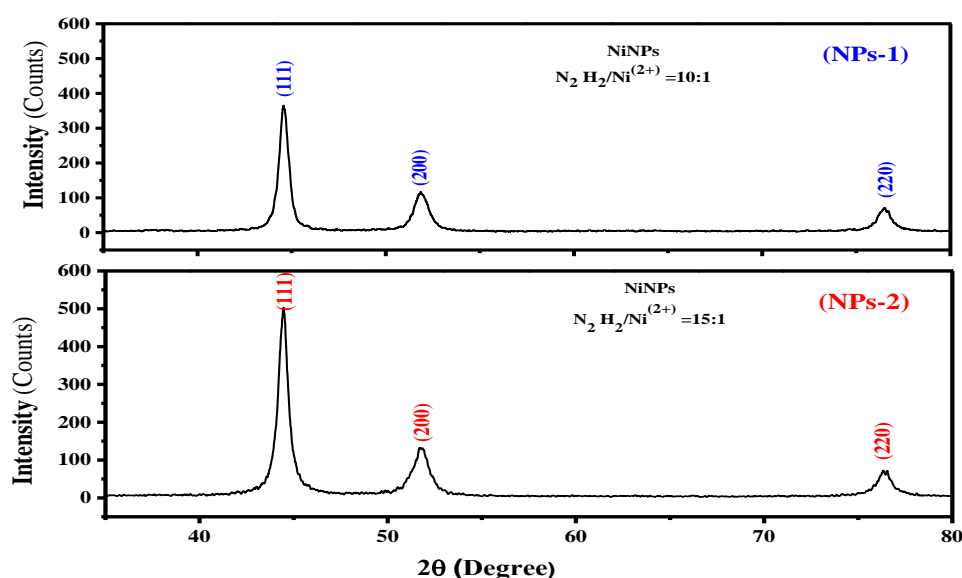


Figure 3. XRD of NPs-1 and NP-2 samples

Furthermore, the average particle size of the nickel nanoparticles, calculated using the Debye-Scherrer

equation, was found to be 12 nm for both molar ratios. X-ray diffraction analysis confirmed the

crystalline structure of the nickel nanoparticles formed through the reduction of Ni²⁺ with hydrazine. These findings are in line with previous reports on the subject references 4 and 12, as shown in Table 1. The d-spacing, lattice parameters, and unit cell

volumes were estimated using the following expressions Eq. 6 and 7

$$d = \frac{\lambda}{2 \sin \theta} \quad \dots\dots 6$$

$$\ln \beta = \ln \frac{k\lambda}{D} + \ln \frac{1}{\cos \theta} \quad \dots\dots 7$$

Table 1. XRD data

samples	2-theta	Miler index	Height	d- space	FWHM	D (nm)	Lactic constant (Å)
NPs-1	44.46029	111	439.76161	2.036064685	0.739	12	3.5265
NPs-2	44.58282	111	332.92147	2.0307529	0.66675	12	3.517

The crystallite size of the nickel nanoparticles was determined using the Scherrer Eq. 6, which involves plotting $\ln \beta$ against $\ln(1/\cos \theta)$ as shown in Fig. 4 (b). The adapted Scherrer relation was used for this analysis. The calculated crystallite sizes of the nickel nanoparticles are presented in Table 1. These values closely align with those obtained from the Scherrer relation, with any slight variations possibly resulting from the averaging of the distribution utilized in the improved Scherrer's plots, which involve the entire XRD peaks²¹.

According to the Williamson-Hall method, both strain and crystallite size have a significant influence on the diffraction lines, leading to their broadening Eq. 8. In the uniform deformation model (UDM), it is assumed that the crystal is isotropic, and therefore,

its properties are independent of the crystallographic orientation along which the measurement is taken.

$$\beta_{hkl} \cos \theta_{hkl} = \frac{k\lambda}{D} + 4\epsilon \sin \theta_{hkl} \dots\dots 8$$

A plot of $\beta_{hkl} \cos \theta_{hkl}$ against $4 \sin \theta_{hkl}$ Describes a linear graph, and the crystallite size (D) and microstrain (ϵ) are individually determined from the line's intercept and slope Fig. 4 (a). The data obtained from XRD is shown in Table 1. The mean crystallite size values computed employing the Scherrer equation, Scherrer plots, and Williamson–Hall forms are virtually identical, implying that the inclusion of strain in the W–H method is changed formulae has negligible impact on the mean (D) value. Nevertheless, the average crystallite sizes calculated applying the Scherrer's and W–H methods exhibit little disparity that can be ascribed to shift in particle size distribution equalizing²¹.

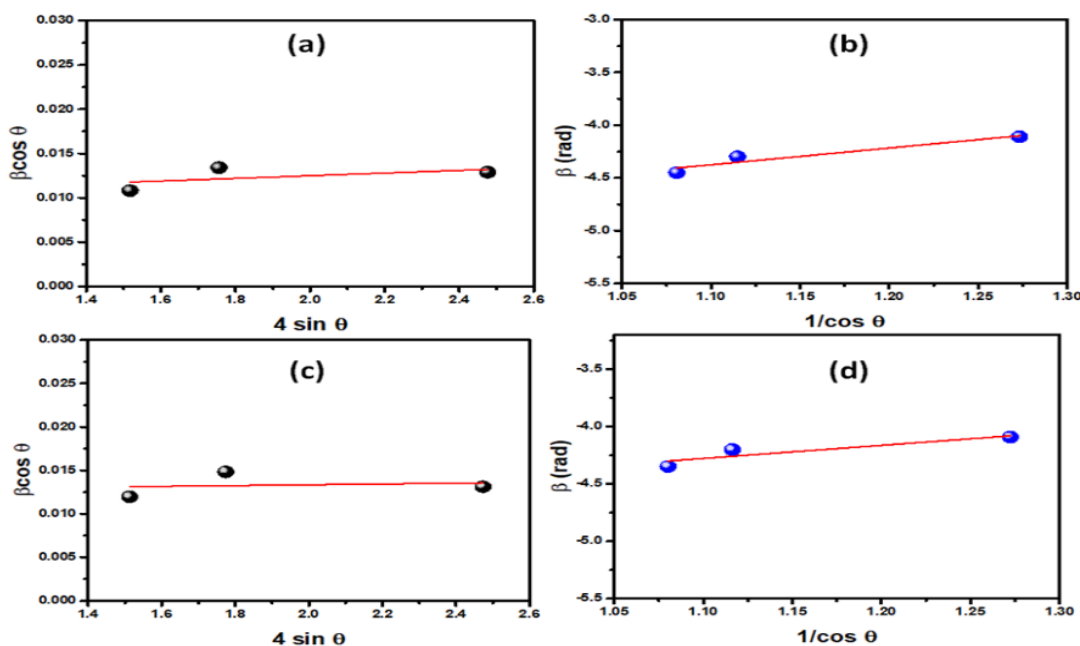


Figure 4. a and c The modified form of Williamson-Hall method. **b and d** linear form of modified Scherrer equation for nickel nanoparticle samples.

Transmission Electron Microscope (TEM)

The TEM images of NPs-1 and NPs-2, with N_2H_2/Ni^{2+} molar ratios of 10:1 and 15:1 respectively, are presented in Figs. 5 and 6. In the case of NPs-1 10:1 ratio, the images reveal a star-like morphology, with an average particle size ranging from 70 to 90 nm. Conversely, NPs-2 15:1 ratio exhibits a different morphology, consisting of monodispersed spherical particles with a smaller average size ranging from 50 to 80 nm. This change in morphology can be

attributed to the influence of the reduction rate on the nucleation process^{22, 23}.

The formation of larger particles with star-like shapes at low hydrazine concentrations can be attributed to the slow reduction rate of nickel chloride. This slower rate leads to the formation of fewer nuclei at the beginning of the reduction reaction. On the other hand, an increase in hydrazine concentration promotes a higher reduction rate, facilitating the generation of a larger number of nuclei and forming smaller nickel nanoparticles^{23, 24}.

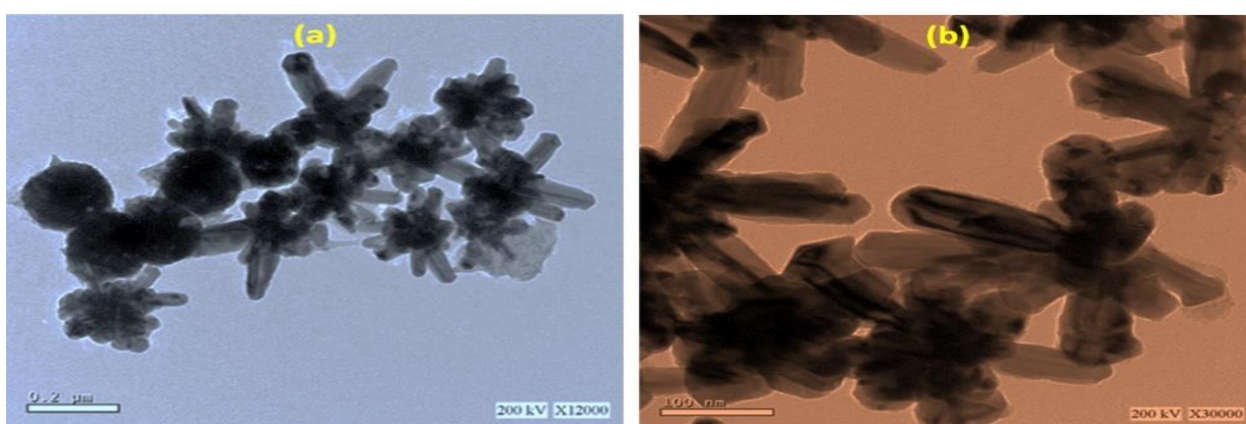


Figure 5. TEM images of NPs-1 at different magnifications; a 2 μ m and b 100 nm.

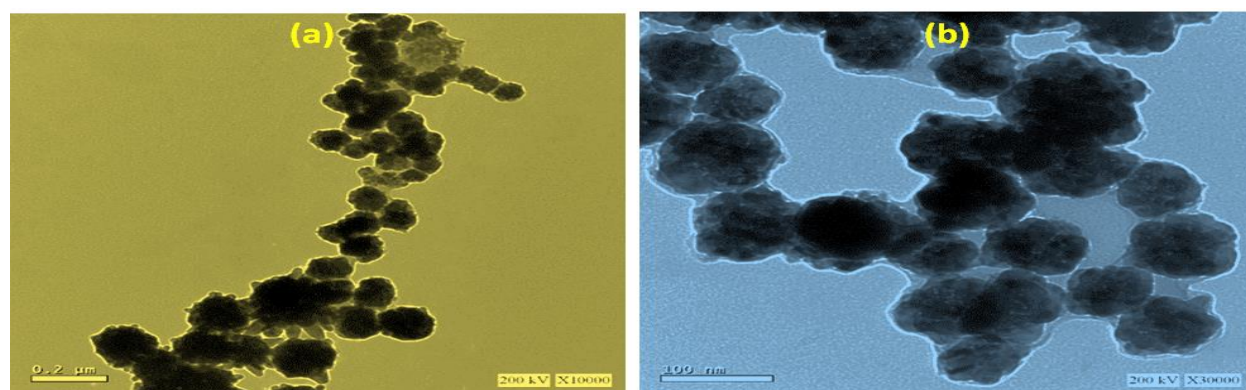


Figure 6. TEM images of NPs-2 at different magnifications a 0.2 μ m and b 100 nm.

Viscosity Reduction of Heavy Crude Oil by NiNPs

Nickel nanoparticle powder was prepared and utilized to recover heavy crude oil. The results demonstrated that the viscosity of the heavy crude oil decreased from 7128 mPa.s to 3495 mPa.s 51% when 0.05% (w/v) of Ni NPs was employed. However, it was observed that the density of the crude oil shifted from 0.9514 g/cm³ to 0.9416 g/cm³, and the API number increased from 17.04 to 18.59 9.0%, indicating the conversion of heavier components into lighter ones. Table 2 illustrates the use of xylene as a solvent in two experiments, with 0.05% Ni NPs

dissolved in xylene. In additional experiments, 1% hydrazine was employed as a hydrogen donor. Fig. 7 showed the viscosity of the crude heavy oil from the Sudan oil plant was reduced to approximately 3495 mPa.s and 3212 mPa.s, respectively, representing a reduction of around 51%, at a temperature of 80°C. This finding aligns with a study conducted by Jadhav²⁵, where they reported that nickel nanoparticles (<100 nm) in conjunction with tetralin solvent under various shear rates (1-1000 s⁻¹) and a concentration of 0.2% wt nickel nanoparticles, facilitated viscosity reduction at high temperatures²⁵. Zhou W¹³ also demonstrated that

nickel ions decreased the activation energy of the process from 16.9 kJ/mol to 10.9 kJ/mol. However, it was observed that the concentrations of oxygenated compounds decreased in the evolved gases while the concentrations of carbon dioxide and water increased¹³.

The high viscosity of heavy oil is primarily attributed to the viscoelastic network formed by compounds such as asphaltene, saturate, aromatic, and resin

aggregations²⁶. Xylene is used as a solvent, while hydrazine acts as a hydrogen donor to enhance the dissolution of asphaltene clusters. The reduction in viscosity is mainly achieved by decreasing the quantity of polar compounds in the oil, which weakens hydrogen bonding²⁷. The effectiveness of nickel nanoparticles as a viscosity reducer is confirmed at a temperature of 80°C with a concentration of 0.05% wt. This concentration yielded the best results for both samples.²⁸

Table 2. Viscosity, density and API reduction results

Sample Name	BS&W (%)		Density (g/cm ³)			Viscosity		
	Water (V%)	Sedi. (V%)	Density (50 °C)	SG API (15°C)	Density Rho (15.6 °C)	API	(mPa.s)	Red. %
Heavy crude oil (Blank)	4.00	0.00	0.9290	0.9530	0.9514	17.04	7128	0.0
1% hydrazine + 3% xylene	4.00	0.00	0.9278	0.9510	0.9502	17.23	6666	6.5
0.05% Ni NPs + 3% xylene	4.00	0.00	0.9190	0.9430	0.9416	18.59	3495	51.0
0.05% Ni NPs + 3% xylene + 1% hydrazine	4.00	0.00	0.9170	0.9410	0.9397	18.89	3212	55.0

* BS= basic sediment, Sedi= sediment . Viscosity applied at 29°C

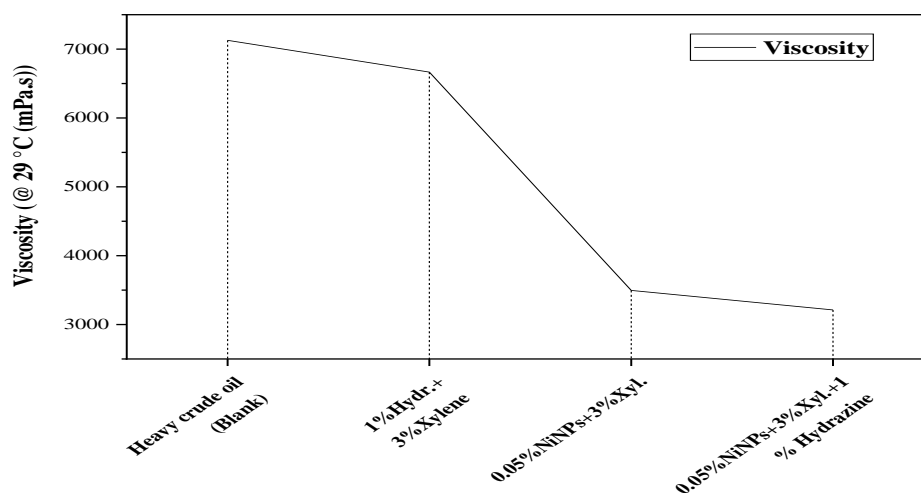


Figure 7. Heavy crude oil viscosity reduction

Conclusion

This study examined the effects of nickel nanoparticles on viscosity reduction in heavy oil through batch-scale experiments. The addition of nanoparticles at a concentration of 0.05% wt, with the assistance of xylene and hydrazine, resulted in a significant reduction in viscosity by 51-55%. However, it was observed that the lighter components of the oil increased during the process. Additionally, introducing nickel nanoparticles led to

a decrease in asphaltene and polar compound content in the oil. This approach shows promise in addressing mechanical stress during oil pumping and transfer.

It is important to note that the study did not explore other parameters such as pH, different concentrations, temperature variations, catalyst doses, and rheological response, which could further

enhance the effectiveness of nickel nanoparticles in viscosity reduction. Nonetheless, these findings contribute valuable insights to the challenge of high viscosity in the Sudan oil field, as there are no

published reports on the role of nickel nanoparticles in reducing oil viscosity. This research expands the existing knowledge and provides opportunities for future investigations in this area.

Acknowledgment

The authors thank The University of Sudan of Science and Technology for their support and facilities. The authors duly acknowledge the

University of Cairo science faculty for providing access to TEM.

Authors' Declaration

- Conflicts of Interest: None.
- We hereby confirm that all the Figures and Tables in the manuscript are ours. Furthermore, any Figures and images, that are not ours, have been included with the necessary permission for re-publication, which is attached to the manuscript.
- No animal studies are present in the manuscript.
- No human studies are present in the manuscript.
- No potentially identified images or data are present in the manuscript.
- Ethical Clearance: The project was approved by the local ethical committee at Sudanese chemical society Khartoum, Khartoum, Sudan.

Authors' Contributions Statement

S. Y. conducted the design, acquisition of data, analysis, M. S. S performed the interpretation,

drafting conception, and B. L. did the revision and proofreading.

References

1. Cao Y, Zhang B, Zhu Z, Rostami M, Dong G, Ling , et al. Access-dispersion-recovery strategy for enhanced mitigation of heavy crude oil pollution using magnetic nanoparticles decorated bacteria. *Bioresour Technol.* 2021 Oct 1; 337: 125404. <https://doi.org/10.1016/j.biortech.2021.125404>
2. Mosavat N, Al-Riyami S, Pourafshary P, Al-Wahaibi Y, Rudyk S. Recovery of viscous and heavy oil by CO₂-saturated brine. *Eng Clim Chang.* 2020 Dec 1; 1: 100009. <https://doi.org/10.1016/j.egycc.2020.100009>
3. Li P, Zhang F, Zhu T, Zhang C, Liu G, Li X. Synthesis and properties of the active polymer for enhanced heavy oil recovery. *Colloids and Surfaces A: Colloids Surf A: Physicochem Eng.* 2021 Oct 5; 626: 127036. <https://doi.org/10.1016/j.colsurfa.2021.127036>
4. Zhou X, Li X, Shen D, Shi L, Zhang Z, Sun X, et al. CO₂ huff-n-puff process to enhance heavy oil recovery and CO₂ storage: An integration study. *Energy.* 2022 Jan 15; 239: 122003. <https://doi.org/10.1016/j.energy.2021.122003>
5. Davoodi SM, Miri S, Taheran M, Brar SK, Galvez-Cloutier R, Martel R. Bioremediation of Unconventional Oil Contaminated Ecosystems under Natural and Assisted Conditions: A Review. *Environ Sci Technol.* 2020 Feb 18; 54(4): 2054-2067. <https://doi.org/10.1021/acs.est.9b00906>
6. Wraight S, Hofmann J, Allpress J, Depro B. *Environmental Justice Concerns and the Proposed Atlantic Coast Pipeline Route in North Carolina .* Research Triangle Park (NC): RTI Press; 2018 <https://doi.org/10.3768/rtipress.2018.mr.0037.1803>
7. Chen S, Liang XJ. Nanobiotechnology and nanomedicine: small change brings big difference. *Sci China Life Sci.* 2018 Apr; 61: 371-2. <https://doi.org/10.1007/s11427-018-9293-2>
8. Janković NZ, Plata DL. Engineered nanomaterials in the context of global element cycles. *Environ Sci Nano.* 2019; 6(9): 2697-2711. <https://doi.org/10.1039/C9EN00322C>
9. Rabiee N, Bagherzadeh M, Ghadiri AM, Kiani M, Ahmadi S, Aldhaher A, et al. High-Gravity-Assisted Green Synthesis of NiO-NPs Anchored on the Surface of Biodegradable Nanobeads with Potential Biomedical Applications. *J Biomed Nanotechnol.* 2020 Apr 1; 16(4): 520-530. <https://doi.org/10.1166/jbn.2020.2904>
10. Ammar SH, Ismail NN, Jabbar MF. Preparation and characterization of magnetic nickel nanoparticles by chemical reduction reaction. *JPRS.* 2018; 8(4): 87-

100. <https://doi.org/10.52716/jprs.v8i4.266>
11. Ádám AA, Szabados M, Varga G, Papp Á, Musza K, Kónya Z, et al. Ultrasound-assisted hydrazine reduction method for the preparation of nickel nanoparticles, physicochemical characterization and catalytic application in Suzuki-Miyaura cross-coupling reaction. *Nanomater.* 2020 Mar 28; 10(4): 632. <https://doi.org/10.3390/nano10040632>
12. Shokrlu YH, Babadagli T. Viscosity reduction of heavy oil/bitumen using micro-and nano-metal particles during aqueous and non-aqueous thermal applications. *J Pet Sci Eng.* 2014 Jul 1; 119: 210-220. <http://dx.doi.org/10.1016/j.petrol.2014.05.012>
13. Zhou W, Xin C, Chen Y, Mouhouadi RD, Chen S. Nanoparticles for Enhancing Heavy Oil Recovery: Recent Progress, Challenges, and Future Perspectives. *Energy Fuel* 2023 May 37 (12): 8057-8078 <https://doi.org/10.1021/acs.energyfuels.3c00684>
14. Rellegadla S, Bairwa HK, Kumari MR, Prajapat G, Nimesh S, Pareek N, et al. An effective approach for enhanced oil recovery using nickel nanoparticles assisted polymer flooding. *Energy Fuel.* 2018 Oct 16; 32(11): 11212-21. <https://doi.org/10.1021/acs.energyfuels.8b02356>
15. Yi S, Babadagli T, Andy Li H. Use of nickel nanoparticles for promoting aquathermolysis reaction during cyclic steam stimulation. *SPE J.* 2018 Feb 14; 23(01): 145-56. <https://doi.org/10.2118/186102-PA>
16. Shakir F, Hussein HQ, Abdulwahhab ZT. Influence of Nanosilica on Solvent Deasphalting for Upgrading Iraqi Heavy Crude Oil . *Baghdad Sci.J .* 2023 Feb. 1 [cited 2023 Jul. 16]; 20(1): 0144. <https://doi.org/10.21123/bsj.2022.6895>
17. Ma L, Zhang S, Zhang X, Dong S, Yu T, Slaný M, et al. Enhanced aquathermolysis of heavy oil catalysed by bentonite supported Fe (III) complex in the present of ethanol. *J Chem Technol Biotechnol.* 2022 May; 97(5): 1128-37. <https://doi.org/10.1002/jctb.6997>
18. Ádám AA, Szabados M, Polyákovics Á, Musza K, Kónya Z. The Synthesis and Use of Nano Nickel Catalysts. *J Nanosci Nanotechnol.* 2019 Jan 1; 19(1): 453-458. <https://doi.org/10.1166/jnn.2019.15781>
19. Usami T, Salman SA, Kuroda K, Gouda MK, Mahdy A, Okido M. Synthesis of Cobalt-Nickel Nanoparticles via a Liquid-Phase Reduction Process. *J Nanotechnol.* 2021 Dec 16; 2021: 1-7. <https://doi.org/10.1155/2021/9401024>
20. Goswami C, Saikia H, Tada K, Tanaka S, Sudarsanam P, Bhargava SK, et al. Bimetallic palladium–nickel nanoparticles anchored on carbon as high-performance electrocatalysts for oxygen reduction and formic acid oxidation reactions. *ACS Appl Energy Mater.* 2020 Sep 2; 3(9): 9285-95. <https://doi.org/10.1021/acsaem.0c01622>
21. Jabir SA, Harbbi KH. A comparative study of Williamson-Hall method and size-strain method through x-ray diffraction pattern of cadmium oxide nanoparticle. In *AIP Conf Proc.* 2020 Dec 15; 2307(1): 020015. AIP Publishing LLC. <https://doi.org/10.1063/5.0033762>
22. Zheng L, Zhang X, Bustillo KC, Yao Y, Zhao L, Zhu M, et al. Growth mechanism of core–shell PtNi–Ni nanoparticles using in situ transmission electron microscopy. *Nanoscale.* 2018; 10(24): 11281-6. <https://doi.org/10.1039/C8NR01625A>
23. Shi Y, Lyu Z, Zhao M, Chen R, Nguyen QN, Xia Y. Noble-metal nanocrystals with controlled shapes for catalytic and electrocatalytic applications. *Chem Rev.* 2020 Jul 15; 121(2): 649-735. <https://doi.org/10.1021/acs.chemrev.0c00454>
24. Bai L, Ouyang Y, Song J, Xu Z, Liu W, Hu J, et al. Synthesis of metallic nanocrystals: from noble metals to base metals. *Mater* 2019 May 8; 12(9): 1497. <https://doi.org/10.3390/ma12091497>
25. Jadhav RM, Kumar G, Balasubramanian N, Sangwai JS. Synergistic effect of nickel nanoparticles with tetralin on the rheology and upgradation of extra heavy oil. *Fuel.* 2022 Jan 15; 308: 122035. <https://doi.org/10.1016/j.fuel.2021.122035>
26. Taborda EA, Alvarado V, Franco CA, Cortés FB. Rheological demonstration of alteration in the heavy crude oil fluid structure upon addition of nanoparticles. *Fuel.* 2017 Feb 1; 189: 322-33. <https://doi.org/10.1016/j.fuel.2016.10.110>
27. Geraldino BR, Nunes RF, Gomes JB, da Poça KS, Giardini I, Silva PV, et al. Evaluation of exposure to toluene and xylene in gasoline station workers. *Adv Prev Med.* 2021 May 20; 2021. <https://doi.org/10.1155/2021/5553633>
28. Farhan RZ, Ebrahim SE. Preparing nanosilica particles from rice husk using precipitation method. *Baghdad Sci J.* 2021; 18: 494-500. <https://doi.org/10.21123/bsj.2021.18.3.0494>

تحسين خواص النفط السوداني باستخدام جسيمات النيكل النانوية

معاذ صديق¹، سهل يسن²، باسنان لال³

¹محلل كيميائي بشركة بترولانرجي المحدودة، السودان.

²الجمعية الكيميائية السودانية، الخرطوم، السودان.

³قسم الكيمياء، جامعة GLA ماتورا، الهند.

الخلاصة

الهدف الأساسي لهذه الدراسة هو تحضير جسيمات النيكل النانوية باستخدام الطرق الكيميائية وذلك بإضافة كيميائيات مختلفة من الهيدرازين كمنتج للإلكترونات بنسب مختلفة في وجود هيدروكسيد الصوديوم كمذيب وذلك لتحسين جودة النفط السوداني بانقاص اللزوجة وزيادة المركبات الخفيفة التي تساعد على الاشتعال. تم تشخيص جسيمات النيكل النانوية باستخدام الأشعة السينية المشتتة و المجهر الإلكتروني النفاذ فائق الدقة. أظهرت النتائج بان جسيمات النيكل النانوية التي تم تحضيرها نقية وكان متوسط حجم الجسيمات في المدى بين 50 إلى 90 نانومتر مع اختلاف حجم الأشكال البلورية اعتمادا على كمية الهيدرازين المختلفة. وجد ان جسيمات النيكل النانوية المحضرة فعالة لانقاص اللزوجة بنسبة 51% من المستوى 7128 إلى 3495 على مقياس اللزوجة بضبط درجة الحرارة إلى 80 درجة مئوية وبجانب اخر نقصت الكثافة من 0.9514 إلى 0.9416 على مقياس الكثافة بحانب زيادة المركبات الخفيفة التي تساعد على الاشتعال من 17.04 إلى 18.59 بحوالي 9%.

الكلمات المفتاحية: السطح الخارجي، جسيمات النيكل النانوية، لزوجة النفط، النفط السوداني، الأشعة السينية المشتتة.